National Geodetic Survey Positioning America for the Future geodesy.noaa.gov

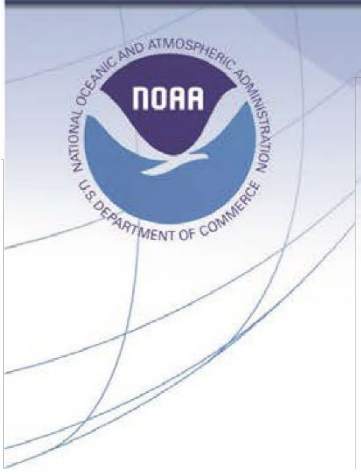

NOAA Technical Memorandum NOS NGS 85

On the Propagation of Formal Error Estimates of Euler Pole Parameters into Modernized NSRS Coordinates

Dru Smith

Silver Spring, MD
September 2020

Versions

Date	Changes
September 8, 2020	Original Release

1 Introduction

The National Geodetic Survey (NGS) is modernizing the National Spatial Reference System (NSRS). As part of that modernization, they will define four terrestrial reference frames which will be mathematically defined relative to the ITRF2020 frame (NGS 2020.) Those four frames are NATRF2022, PATRF2022, CATRF2022 and MATRF2022 (named for the North American, Pacific, Caribbean and Mariana plates, respectively.)

As mentioned by NGS (ibid), the defining relationship between time-dependent Cartesian coordinates in ITRF2020 and time-dependent Cartesian coordinates in each of the four terrestrial reference frames will be through a 3 × 3 rotation matrix, generically written as:

$$\begin{bmatrix} X(t) \\ Y(t) \\ Z(t) \end{bmatrix}_F = R_{F,I}(t, t_0) \begin{bmatrix} X(t) \\ Y(t) \\ Z(t) \end{bmatrix}_I \tag{1}$$

Where *F* is a general variable meaning "some plate fixed frame", which could be NATRF2022, PATRF2022, CATRF2022 or MATRF2022 in the modernized NSRS. The *I* stands for ITRF2020. The value "t_0" will be set to 2020.00 (ibid).

Also as stated in NGS (ibid), all geometric coordinate computations will be performed in XYZ in the ITRF2020 first, and then transformed to NATRF2022, PATRF2022, CATRF2022 and MATRF2022, using equation 1 (above). However, to do so requires not only Equation 1 (for transforming the coordinates), but also a companion equation for computing the *uncertainties* of coordinates.

However, since both ITRF2020 XYZ coordinates and the Euler pole parameters (EPPs) found in the *R* matrix have uncertainties, this raises the question of how, and whether, to fully propagate *both* of those uncertainties into NATRF2022, PATRF2022, CATRF2022 and MATRF2022 XYZ coordinates. Those questions are the topic of this paper.

2 Error Propagation

The rules of error propagation are well established. Yet for practical reasons, which will be covered soon, NGS must carefully consider whether they will be followed *in their entirety* for the modernized NSRS, particularly with regard to the propagation of EPP uncertainties into modernized NSRS coordinates.

Before discussing whether to fully propagate errors, we begin by formally deriving the error propagation equations of interest to this study.

The *R* matrix in equation 1 is (NGS, 2020; Equation 60):

$$R_{F,I}(t, t_0) = \begin{bmatrix} 1 & \Delta t(\dot{\omega}_Z)_{F,I} & -\Delta t(\dot{\omega}_Y)_{F,I} \\ -\Delta t(\dot{\omega}_Z)_{F,I} & 1 & \Delta t(\dot{\omega}_X)_{F,I} \\ \Delta t(\dot{\omega}_Y)_{F,I} & -\Delta t(\dot{\omega}_X)_{F,I} & 1 \end{bmatrix} \tag{2}$$

where $\Delta t = (t - t_0)$. Inserting this into equation 1, and re-arranging, yields the following:

$$\begin{bmatrix} X(t) \\ Y(t) \\ Z(t) \end{bmatrix}_F = \begin{bmatrix} 1 & \Delta t(\dot{\omega}_Z)_{F,I} & -\Delta t(\dot{\omega}_Y)_{F,I} \\ -\Delta t(\dot{\omega}_Z)_{F,I} & 1 & \Delta t(\dot{\omega}_X)_{F,I} \\ \Delta t(\dot{\omega}_Y)_{F,I} & -\Delta t(\dot{\omega}_X)_{F,I} & 1 \end{bmatrix} \begin{bmatrix} X(t) \\ Y(t) \\ Z(t) \end{bmatrix}_I = \begin{bmatrix} X_I(t) + Y_I(t)\Delta t(\dot{\omega}_Z)_{F,I} - Z_I(t)\Delta t(\dot{\omega}_Y)_{F,I} \\ -X_I(t)\Delta t(\dot{\omega}_Z)_{F,I} + Y_I(t) + Z_I(t)\Delta t(\dot{\omega}_X)_{F,I} \\ X_I(t)\Delta t(\dot{\omega}_Y)_{F,I} - Y_I(t)\Delta t(\dot{\omega}_X)_{F,I} + Z_I(t) \end{bmatrix} \quad (3)$$

The six stochastic variables, that is the variables which have formal uncertainties associated with them, are the three ITRF2020 coordinates, $X_I(t)$, $Y_I(t)$, $Z_I(t)$ and the three micro-rotation rates relating the plate-fixed frame to ITRF2020, $(\dot{\omega}_X)_{F,I}$, $(\dot{\omega}_Y)_{F,I}$, $(\dot{\omega}_Z)_{F,I}$. Unfortunately, equation 3 is non-linear in those six variables. This doesn't prevent error propagation; it only makes it somewhat more complicated.

To begin addressing that, we define the six stochastic variables as vector $\boldsymbol{X}$ (comprised of two sub-vectors $\boldsymbol{X_1}$ and $\boldsymbol{X_2}$) and our three, to-be-determined, plate-fixed frame Cartesian coordinates as vector $\boldsymbol{Y}$:

$$\boldsymbol{X} = \begin{bmatrix} \boldsymbol{X_1} \\ \boldsymbol{X_2} \end{bmatrix} = \begin{bmatrix} X_I(t) \\ Y_I(t) \\ Z_I(t) \\ (\dot{\omega}_X)_{F,I} \\ (\dot{\omega}_Y)_{F,I} \\ (\dot{\omega}_Z)_{F,I} \end{bmatrix} \quad (4)$$

$$\boldsymbol{Y} = \begin{bmatrix} X_F(t) \\ Y_F(t) \\ Z_F(t) \end{bmatrix} \quad (5)$$

This allows us to write the non-linear Equation 3 as:

$$\boldsymbol{Y}(\boldsymbol{X}) = \begin{bmatrix} X_F\left(X_I, Y_I, Z_I, (\dot{\omega}_Y)_{F,I}, (\dot{\omega}_Z)_{F,I}\right) \\ Y_F\left(X_I, Y_I, Z_I, (\dot{\omega}_X)_{F,I}, (\dot{\omega}_Z)_{F,I}\right) \\ Z_F\left(X_I, Y_I, Z_I, (\dot{\omega}_X)_{F,I}, (\dot{\omega}_Y)_{F,I}\right) \end{bmatrix} \quad (6)$$

We now introduce the 6 × 6 dispersion matrix for the pre-determined $\boldsymbol{X}$ vector as $\boldsymbol{\Sigma_X}$. This matrix will be block-diagonal and known. The lower right 3 × 3 block will be dispersions for the micro-rotation rates (Σ_{X_2}) and will be part of the definition of the plate fixed frame in the modernized NSRS. These values will be identical every time we use them. The upper left 3 × 3 block will be dispersion for the ITRF2020 Cartesian coordinates (Σ_{X_1}) and will come from OPUS[1] in processing a GNSS file (and will be dependent upon the point surveyed, the data

[1] NGS's Online Positioning User Service <https://www.ngs.noaa.gov/OPUS/>

collected, the version of OPUS used, the Continuously Operating Reference Stations (CORSs) chosen, etc.) That is:

$$\boldsymbol{\Sigma_X} = \begin{bmatrix} \Sigma_{X_1} & \mathbf{0} \\ \mathbf{0} & \Sigma_{X_2} \end{bmatrix} = \begin{bmatrix} \boldsymbol{\sigma}^2_{X_I(t)} & \boldsymbol{\sigma}_{X_I(t),Y_I(t)} & \boldsymbol{\sigma}_{X_I(t),Z_I(t)} & & \mathbf{0} & \\ \boldsymbol{\sigma}_{Y_I(t),X_I(t)} & \boldsymbol{\sigma}^2_{Y_I(t)} & \boldsymbol{\sigma}_{Y_I(t),Z_I(t)} & & & \\ \boldsymbol{\sigma}_{Z_I(t),X_I(t)} & \boldsymbol{\sigma}_{Z_I(t),Y_I(t)} & \boldsymbol{\sigma}^2_{Z_I(t)} & & & \\ & & & \boldsymbol{\sigma}^2_{(\dot{\omega}_X)_{F,I}} & \boldsymbol{\sigma}_{(\dot{\omega}_X)_{F,I},(\dot{\omega}_Y)_{F,I}} & \boldsymbol{\sigma}_{(\dot{\omega}_X)_{F,I},(\dot{\omega}_Z)_{F,I}} \\ & \mathbf{0} & & \boldsymbol{\sigma}_{(\dot{\omega}_Y)_{F,I},(\dot{\omega}_X)_{F,I}} & \boldsymbol{\sigma}^2_{(\dot{\omega}_Y)_{F,I}} & \boldsymbol{\sigma}_{(\dot{\omega}_Y)_{F,I},(\dot{\omega}_Z)_{F,I}} \\ & & & \boldsymbol{\sigma}_{(\dot{\omega}_Z)_{F,I},(\dot{\omega}_X)_{F,I}} & \boldsymbol{\sigma}_{(\dot{\omega}_Z)_{F,I},(\dot{\omega}_Y)_{F,I}} & \boldsymbol{\sigma}^2_{(\dot{\omega}_Z)_{F,I}} \end{bmatrix} \tag{7}$$

We now introduce the 3 × 3 dispersion matrix for the desired $\boldsymbol{Y}$ vector as $\boldsymbol{\Sigma_Y}$. This matrix is unknown and sought. It is computable using a Jacobian matrix ($\boldsymbol{J}$) to apply the law of error propagation to the non-linear equation 6, as:

$$\boldsymbol{\Sigma_Y} = \boldsymbol{J}\boldsymbol{\Sigma_X}\boldsymbol{J}^{\boldsymbol{T}} \tag{8}$$

Where

$$J = \frac{\partial \boldsymbol{Y}(\boldsymbol{X})}{\partial \boldsymbol{X}^T} = \begin{bmatrix} \frac{\partial X_F(t)}{\partial X_I(t)} & \frac{\partial X_F(t)}{\partial Y_I(t)} & \frac{\partial X_F(t)}{\partial Z_I(t)} & \frac{\partial X_F(t)}{\partial (\dot{\omega}_X)_{F,I}} & \frac{\partial X_F(t)}{\partial (\dot{\omega}_Y)_{F,I}} & \frac{\partial X_F(t)}{\partial (\dot{\omega}_Z)_{F,I}} \\ \frac{\partial Y_F(t)}{\partial X_I(t)} & \frac{\partial Y_F(t)}{\partial Y_I(t)} & \frac{\partial Y_F(t)}{\partial Z_I(t)} & \frac{\partial Y_F(t)}{\partial (\dot{\omega}_X)_{F,I}} & \frac{\partial Y_F(t)}{\partial (\dot{\omega}_Y)_{F,I}} & \frac{\partial Y_F(t)}{\partial (\dot{\omega}_Z)_{F,I}} \\ \frac{\partial Z_F(t)}{\partial X_I(t)} & \frac{\partial Z_F(t)}{\partial Y_I(t)} & \frac{\partial Z_F(t)}{\partial Z_I(t)} & \frac{\partial Z_F(t)}{\partial (\dot{\omega}_X)_{F,I}} & \frac{\partial Z_F(t)}{\partial (\dot{\omega}_Y)_{F,I}} & \frac{\partial Z_F(t)}{\partial (\dot{\omega}_Z)_{F,I}} \end{bmatrix} =$$

$$\begin{bmatrix} 1 & \Delta t(\dot{\omega}_Z)_{F,I} & -\Delta t(\dot{\omega}_Y)_{F,I} & 0 & -Z_I(t)\Delta t & Y_I(t)\Delta t \\ -\Delta t(\dot{\omega}_Z)_{F,I} & 1 & \Delta t(\dot{\omega}_X)_{F,I} & Z_I(t)\Delta t & 0 & -X_I(t)\Delta t \\ \Delta t(\dot{\omega}_Y)_{F,I} & -\Delta t(\dot{\omega}_X)_{F,I} & 1 & -Y_I(t)\Delta t & X_I(t)\Delta t & 0 \end{bmatrix} = \tag{9}$$

$$\Delta t \begin{bmatrix} 1/\Delta t & (\dot{\omega}_Z)_{F,I} & -(\dot{\omega}_Y)_{F,I} & 0 & -Z_I(t) & Y_I(t) \\ -(\dot{\omega}_Z)_{F,I} & 1/\Delta t & (\dot{\omega}_X)_{F,I} & Z_I(t) & 0 & -X_I(t) \\ (\dot{\omega}_Y)_{F,I} & -(\dot{\omega}_X)_{F,I} & 1/\Delta t & -Y_I(t) & X_I(t) & 0 \end{bmatrix}$$

Applying equation 9 to equation 8, and relying upon the block-diagonal nature of the $\boldsymbol{\Sigma_X}$ matrix, one arrives at:

$$
\begin{aligned}
\boldsymbol{\Sigma_Y} &= \\
&= (\Delta t)^2 \begin{bmatrix} \left(\frac{1}{\Delta t}\right) & (\dot{\omega}_Z)_{F,I} & -(\dot{\omega}_Y)_{F,I} \\ -(\dot{\omega}_Z)_{F,I} & \left(\frac{1}{\Delta t}\right) & (\dot{\omega}_X)_{F,I} \\ (\dot{\omega}_Y)_{F,I} & -(\dot{\omega}_X)_{F,I} & \left(\frac{1}{\Delta t}\right) \end{bmatrix} \Sigma_{X_1} \begin{bmatrix} \left(\frac{1}{\Delta t}\right) & (\dot{\omega}_Z)_{F,I} & -(\dot{\omega}_Y)_{F,I} \\ -(\dot{\omega}_Z)_{F,I} & \left(\frac{1}{\Delta t}\right) & (\dot{\omega}_X)_{F,I} \\ (\dot{\omega}_Y)_{F,I} & -(\dot{\omega}_X)_{F,I} & \left(\frac{1}{\Delta t}\right) \end{bmatrix}^{\boldsymbol{T}} \\
&\quad + (\Delta t)^2 \begin{bmatrix} 0 & -Z_I(t) & Y_I(t) \\ Z_I(t) & 0 & -X_I(t) \\ -Y_I(t) & X_I(t) & 0 \end{bmatrix} \Sigma_{X_2} \begin{bmatrix} 0 & -Z_I(t) & Y_I(t) \\ Z_I(t) & 0 & -X_I(t) \\ -Y_I(t) & X_I(t) & 0 \end{bmatrix}^{\boldsymbol{T}} \\
&= (\Delta t)^2 \begin{bmatrix} \left(\frac{1}{\Delta t}\right) & (\dot{\omega}_Z)_{F,I} & -(\dot{\omega}_Y)_{F,I} \\ -(\dot{\omega}_Z)_{F,I} & \left(\frac{1}{\Delta t}\right) & (\dot{\omega}_X)_{F,I} \\ (\dot{\omega}_Y)_{F,I} & -(\dot{\omega}_X)_{F,I} & \left(\frac{1}{\Delta t}\right) \end{bmatrix} \begin{bmatrix} \boldsymbol{\sigma}^2_{X_I(t)} & \boldsymbol{\sigma}_{X_I(t),Y_I(t)} & \boldsymbol{\sigma}_{X_I(t),Z_I(t)} \\ \boldsymbol{\sigma}_{Y_I(t),X_I(t)} & \boldsymbol{\sigma}^2_{Y_I(t)} & \boldsymbol{\sigma}_{Y_I(t),Z_I(t)} \\ \boldsymbol{\sigma}_{Z_I(t),X_I(t)} & \boldsymbol{\sigma}_{Z_I(t),Y_I(t)} & \boldsymbol{\sigma}^2_{Z_I(t)} \end{bmatrix} \begin{bmatrix} \left(\frac{1}{\Delta t}\right) & (\dot{\omega}_Z)_{F,I} & -(\dot{\omega}_Y)_{F,I} \\ -(\dot{\omega}_Z)_{F,I} & \left(\frac{1}{\Delta t}\right) & (\dot{\omega}_X)_{F,I} \\ (\dot{\omega}_Y)_{F,I} & -(\dot{\omega}_X)_{F,I} & \left(\frac{1}{\Delta t}\right) \end{bmatrix}^{\boldsymbol{T}} \\
&\quad + (\Delta t)^2 \begin{bmatrix} 0 & -Z_I(t) & Y_I(t) \\ Z_I(t) & 0 & -X_I(t) \\ -Y_I(t) & X_I(t) & 0 \end{bmatrix} \begin{bmatrix} \boldsymbol{\sigma}^2_{(\dot{\omega}_X)_{F,I}} & \boldsymbol{\sigma}_{(\dot{\omega}_X)_{F,I},(\dot{\omega}_Y)_{F,I}} & \boldsymbol{\sigma}_{(\dot{\omega}_X)_{F,I},(\dot{\omega}_Z)_{F,I}} \\ \boldsymbol{\sigma}_{(\dot{\omega}_Y)_{F,I},(\dot{\omega}_X)_{F,I}} & \boldsymbol{\sigma}^2_{(\dot{\omega}_Y)_{F,I}} & \boldsymbol{\sigma}_{(\dot{\omega}_Y)_{F,I},(\dot{\omega}_Z)_{F,I}} \\ \boldsymbol{\sigma}_{(\dot{\omega}_Z)_{F,I},(\dot{\omega}_X)_{F,I}} & \boldsymbol{\sigma}_{(\dot{\omega}_Z)_{F,I},(\dot{\omega}_Y)_{F,I}} & \boldsymbol{\sigma}^2_{(\dot{\omega}_Z)_{F,I}} \end{bmatrix} \begin{bmatrix} 0 & -Z_I(t) & Y_I(t) \\ Z_I(t) & 0 & -X_I(t) \\ -Y_I(t) & X_I(t) & 0 \end{bmatrix}^{\boldsymbol{T}} \\
&= \boldsymbol{\Sigma_{Y_1}} + \boldsymbol{\Sigma_{Y_2}}
\end{aligned}
\tag{10}
$$

Where $\boldsymbol{\Sigma_{Y_1}}$ is that portion of NSRS XYZ coordinate uncertainty due to ITRF2020 XYZ positioning uncertainty ($\boldsymbol{\Sigma_{X_1}}$), while $\boldsymbol{\Sigma_{Y_2}}$ is that portion of NSRS XYZ uncertainty due to EPP2022 uncertainty ($\boldsymbol{\Sigma_{X_2}}$).

Equation 10 is elegant for a few reasons. First it allows us to separate the impact of the ITRF2020 XYZ positioning uncertainty (from GNSS processing software like OPUS, in green) from the impact of EPP errors (as defined by the modernized NSRS, in blue). These two impacts should (formally) be combined to create the error estimates of the plate-fixed NSRS XYZ coordinates.

If NGS were to perform formal error propagation to determine the mathematically correct error estimates to apply to plate-fixed XYZ coordinates in the modernized NSRS, then Equation 10 would be the way to go. However, there is a practical side which must be considered in contrast to mathematical correctness, and which will be investigated in Chapter 3. Before considering that, however, we must first consider error estimates among different types of coordinates.

2.1 ϕλh vs ENU vs XYZ

While NGS software will work primarily with XYZ coordinates when performing geometric computations and adjustments, the final results as presented to users will also be in the ϕλh system, as those coordinates are more intuitive and more frequently needed by users of the NSRS. Therefore, a version of Equation 10 needs to be derived in the ϕλh system. Before proceeding with that derivation though, consider this practical aspect: most users will wish to know their coordinate uncertainty in *linear* units. That is, since ϕ and λ are in *curvilinear* (radians, decimal degrees, degrees/minutes/seconds, etc.) units, their uncertainties will also be in these units. Since most users desire a linear unit (meters, feet, etc.), often to a projected coordinate system (such as State Plane) a conversion will need to take place. Usually that conversion yields uncertainties in the East, North and Up directions (ENU system). Rather than derive the uncertainty in curvilinear units and then convert, just consider that the uncertainty in the XYZ system and the uncertainty in the ENU system are related through a simple three step rotation that rotates the XYZ axes so that X points east Y points north and Z points up.

This is best seen by writing out the equation for coordinates in the XYZ axes versus the ENU axes. First, note that the ENU axes are dependent upon choosing some point on the surface of the Earth with latitude and longitude ϕ_0 and λ_0. Now let's define ENU coordinates in terms of XYZ so we can derive the relationship between their dispersions.

$$\begin{bmatrix} E \\ N \\ U \end{bmatrix} = \begin{bmatrix} \cos(\pi/2) & \sin(\pi/2) & 0 \\ -\sin(\pi/2) & \cos(\pi/2) & 0 \\ 0 & 0 & 1 \end{bmatrix} \begin{bmatrix} \sin\phi_0 & 0 & -\cos\phi_0 \\ 0 & 1 & 0 \\ \cos\phi_0 & 0 & \sin\phi_0 \end{bmatrix} \begin{bmatrix} \cos\lambda_0 & \sin\lambda_0 & 0 \\ -\sin\lambda_0 & \cos\lambda_0 & 0 \\ 0 & 0 & 1 \end{bmatrix} \begin{bmatrix} X \\ Y \\ Z \end{bmatrix} + \begin{bmatrix} T_X \\ T_Y \\ T_Z \end{bmatrix} \quad (11)$$

Where the $[T_X,T_Y,T_Z]^T$ vector is the translation vector from the ITRF origin up to point (ϕ_0,λ_0). This equation simplifies down to the following form:

$$\begin{bmatrix} E \\ N \\ U \end{bmatrix} = \begin{bmatrix} -\sin\lambda_0 & \cos\lambda_0 & 0 \\ -\cos\lambda_0\sin\phi_0 & -\sin\lambda_0\sin\phi_0 & \cos\phi_0 \\ \cos\lambda_0\cos\phi_0 & \cos\phi_0\sin\lambda_0 & \sin\phi_0 \end{bmatrix} \begin{bmatrix} X \\ Y \\ Z \end{bmatrix} + \begin{bmatrix} T_X \\ T_Y \\ T_Z \end{bmatrix} \quad (12)$$

Now we consider the Jacobian matrix, being the derivative of ENU relative to XYZ and the see that the translations fall out, so that:

$$J_{XYZ2ENU} = \frac{\partial \begin{bmatrix} E \\ N \\ U \end{bmatrix}}{\partial \begin{bmatrix} X \\ Y \\ Z \end{bmatrix}^T} = \begin{bmatrix} -\sin\lambda_0 & \cos\lambda_0 & 0 \\ -\cos\lambda_0\sin\phi_0 & -\sin\lambda_0\sin\phi_0 & \cos\phi_0 \\ \cos\lambda_0\cos\phi_0 & \cos\phi_0\sin\lambda_0 & \sin\phi_0 \end{bmatrix} \quad (13)$$

Note that the Jacobian for the reverse transformation is equal to the inverse (as well as the transpose) of the above matrix:

$$J_{ENU2XYZ} = \frac{\partial \begin{bmatrix} X \\ Y \\ Z \end{bmatrix}}{\partial \begin{bmatrix} E \\ N \\ U \end{bmatrix}^T} = \begin{bmatrix} -\sin\lambda_0 & -\cos\lambda_0 \sin\phi_0 & \cos\lambda_0 \cos\phi_0 \\ \cos\lambda_0 & -\sin\lambda_0 \sin\phi_0 & \cos\phi_0 \sin\lambda_0 \\ 0 & \cos\phi_0 & \sin\phi_0 \end{bmatrix} \tag{14}$$

Now it's easy to relate dispersions in the ENU system relative to the XYZ system, and vice versa. Let's use $\boldsymbol{\Sigma_E}$ as the dispersion matrix for the ENU coordinates:

$$\Sigma_E = J_{XYZ2ENU}\Sigma_Y {J^T}_{XYZ2ENU} = \begin{bmatrix} -\sin\lambda_0 & \cos\lambda_0 & 0 \\ -\cos\lambda_0 \sin\phi_0 & -\sin\lambda_0 \sin\phi_0 & \cos\phi_0 \\ \cos\lambda_0 \cos\phi_0 & \cos\phi_0 \sin\lambda_0 & \sin\phi_0 \end{bmatrix} \Sigma_Y \begin{bmatrix} -\sin\lambda_0 & \cos\lambda_0 & 0 \\ -\cos\lambda_0 \sin\phi_0 & -\sin\lambda_0 \sin\phi_0 & \cos\phi_0 \\ \cos\lambda_0 \cos\phi_0 & \cos\phi_0 \sin\lambda_0 & \sin\phi_0 \end{bmatrix}^T \tag{15}$$

And similarly:

$$\Sigma_Y = J_{ENU2XYZ}\Sigma_E {J^T}_{ENU2XYZ} = \begin{bmatrix} -\sin\lambda_0 & -\cos\lambda_0 \sin\phi_0 & \cos\lambda_0 \cos\phi_0 \\ \cos\lambda_0 & -\sin\lambda_0 \sin\phi_0 & \cos\phi_0 \sin\lambda_0 \\ 0 & \cos\phi_0 & \sin\phi_0 \end{bmatrix} \Sigma_E \begin{bmatrix} -\sin\lambda_0 & -\cos\lambda_0 \sin\phi_0 & \cos\lambda_0 \cos\phi_0 \\ \cos\lambda_0 & -\sin\lambda_0 \sin\phi_0 & \cos\phi_0 \sin\lambda_0 \\ 0 & \cos\phi_0 & \sin\phi_0 \end{bmatrix}^T \tag{16}$$

Therefore, a combination of Equation 10 and Equation 15 can be used to quantify the uncertainties in ENU based upon XYZ uncertainties in ITRF2020 and uncertainties in the EPPs of any given plate/frame.

3 Numerical Examples

In the modernized NSRS, the EPP2022 model will contain the Euler pole parameters, and their uncertainties for the four plate-fixed frames of NATRF2022, PATRF2022, CATRF2022 and MATRF2022. The EPP2022 parameters will be estimated such that rotations due to tectonic plate motion of the North American, Pacific, Caribbean and Mariana plates are minimized within their respective frames, for select points on the plates (e.g. possibly not in areas of active deformation.)

While the final values that will comprise EPP2022 are not yet known, there are current best estimates for all of them which can serve as proxies for some numerical examples. The table below lists the values which will be used in this study, with the "F/I" subscript dropped for readability. In the modernized NSRS, all of these values will refer to ITRF2020, but for these numerical examples, only the most recently known ITRF value for each plate is used. Micro-rotation rates and their standard deviations are in milliarcseconds per year (mas/y), while covariances are in $(\text{mas/y})^2$.

Table 1: Current best estimates of Euler pole parameters for the four tectonic plates associated with the four frames of the modernized NSRS

	North America	Pacific	Caribbean(1)	Caribbean(2)	Mariana
$\dot{\omega}_X$	0.024	-0.409	0.049	-0.072	-8.089
$\dot{\omega}_Y$	-0.694	1.047	-1.088	-0.933	5.937

$\dot{\omega}_Z$	-0.063	-2.169	0.664	0.596	2.159
$\boldsymbol{\sigma}_{\dot{\omega}_X}$	±0.002	±0.003	±0.201	±0.006	±0.416
$\boldsymbol{\sigma}_{\dot{\omega}_Y}$	±0.005	±0.004	±0.417	±0.012	±0.288
$\boldsymbol{\sigma}_{\dot{\omega}_Z}$	±0.004	±0.004	±0.146	±0.004	±0.133
$\boldsymbol{\sigma}_{\dot{\omega}_X,\dot{\omega}_Y}$	0*	0*	0*	0*	-0.120**
$\boldsymbol{\sigma}_{\dot{\omega}_X,\dot{\omega}_Z}$	0*	0*	0*	0*	-0.055**
$\boldsymbol{\sigma}_{\dot{\omega}_Y,\dot{\omega}_Z}$	0*	0*	0*	0*	0.038**
Reference Frame	ITRF2014	ITRF2014	ITRF2008	IGS14	ITRF2014
Source	Altamimi et al, 2017	Altamimi et al, 2017	Altamimi, Métivier and Collilieux, 2012	Snay and Saleh, 2020	Smith, 2020

* These values are not likely to be zero, but were not available from the source listed.
** These values were not available in the source as published

Two different estimates of the Caribbean EPPs are provided. This is because they have such radically different uncertainties that it was deemed interesting to see how the difference in these EPP uncertainties would actually impact different NSRS coordinate uncertainties in the two different cases.

Before proceeding, it is worth noting the approximately two orders of magnitude difference between the standard deviations for the EPPs of the North American & Pacific plates versus those for the Caribbean(1) & Mariana estimates. These orders of magnitude (and the Mariana in particular) will be a crucial part of the final discussion.

If ITRF2020 *XYZ* values, and Δt were available, numerical tests of equation 12 could be performed. Therefore, a handful of representative locations were chosen on each plate for the purposes of providing simple ITRF2020 coordinates across each plate. These are listed in the table below. The latitude and longitude are the ITRF2020 (and also N/P/C/MATRF2022) coordinates at 2020.0. The point name is just a simple descriptor and does not represent any specific geodetic control point.

Table 2: Points tested for each plate

Plate	Point Name	Latitude	Longitude
North American	Northern Alaska	72°	205°
	Northern Canada	75°	270°
	Greenland	80°	320°
	Washington State	45°	240°
	Maine	45°	290°
	Gulf Coast	30°	270°
	Mexico City	19°	261°
Pacific	Hawaii	19.5°	205°
	American Samoa	-14.3°	189.25°

Caribbean	NW Puerto Rico	18.4°	292.8°
	St. Croix, USVI	17.7°	295.2°
Mariana	Guam	13.5°	144.75°
	Saipan	15.2°	145.75°
	Farallon de Pajaros	20.55°	144.9°

A computer program[2] was written to do the following:

- Pick a plate/frame
- Select points of interest (see Table 2 above)
- Assuming no ellipsoid height, compute X,Y and Z for the selected points
- Assign a simple dispersion for these XYZ coordinates (based upon a +/- 1 cm standard deviation in the E and N directions, a 3 cm standard deviation in the U direction, no correlations and equation 16)
- Set t_0=2020
- Look back 100 years (to t=1920), in 1 year intervals, and then begin looping t forward, letting the plate rotate at its given rate until t=2120.
    - At every time t, compute the new ITRF2020 X,Y,Z values
    - Assign the same simple 1/1/3 cm ENU standard deviation values as before (see above) to simulate a date-independent positioning uncertainty estimate for ITRF2020 XYZ coordinates, using equation 16
    - Apply equation 10 to yield the dispersions of (N/P/C/M)ATRF2022 XYZ coordinates at t
        - Separating the impacts of ITRF2020 XYZ positioning uncertainties from EPP2022 uncertainties
    - Apply equation 15 to yield the dispersions of (N/P/C/M)ATRF2022 ENU coordinates at t, separating the impacts of ITRF2020 XYZ uncertainties from EPP2022 uncertainties
    - Report out how the two different uncertainties impact the ENU uncertainties in (N/P/C/M)ATRF2022

The first, and immediate conclusion which became apparent from this program was that the positioning uncertainties in the NSRS coordinates ($\boldsymbol{\Sigma}_{\boldsymbol{Y_1}}$), were numerically identical to the positioning uncertainties in the ITRF ($\boldsymbol{\Sigma}_{\boldsymbol{X_1}}$). That is, with a 1/1/3 cm standard deviation in ENU in the ITRF, this always computed to 1/1/3 cm standard deviation in ENU uncertainty in the NSRS (and, when converted to XYZ, the numbers, of course, remained identical) This conclusion holds whether the off-diagonal elements are set to zero or non-zero values. Therefore, the only real questions remaining were: (1) what impact did the EPP uncertainty ($\boldsymbol{\Sigma}_{\boldsymbol{X_2}}$) have on NSRS coordinate uncertainty ($\boldsymbol{\Sigma}_{\boldsymbol{Y_2}}$) and (2) should we formally apply that?

[2] /home/dru/Euler/eppsigs2coordsigs.f. The program is too long for inclusion here, but is available by request of the author.

The answer to the first question is found in the table below.

Table 3: Formally propagated total horizontal uncertainty due solely to EPP uncertainties (cm)

Frame	Point	1 year	10 years	100 years
NATRF2022 (using Altamimi et al 2017)	1 – Northern Alaska	0.04	0.37	3.7
	2 – Northern Canada	0.04	0.37	3.7
	3 - Greenland	0.04	0.37	3.7
	4 – Washington State	0.04	0.36	3.6
	5 - Maine	0.04	0.36	3.6
	6 – Gulf Coast	0.04	0.36	3.6
	7 – Mexico City	0.04	0.35	3.5
PATRF2022 (using Altamimi et al 2017)	1 - Hawaii	0.03	0.35	3.5
	2 – American Samoa	0.03	0.35	3.5
CATRF2022 (using Altamimi et al 2012)	1 – NW Puerto Rico	0.95	9.52	95.2
	2 – St. Croix, USVI	0.97	9.66	96.6
CATRF2022 (using Snay and Saleh 2020)	1 – NW Puerto Rico	0.03	0.28	2.8
	2 – St. Croix, USVI	0.03	0.28	2.7
MATRF2022 (using Smith, 2020)	1 - Guam	1.29	12.90	129.0
	2 - Saipan	1.29	12.89	128.9
	3 – Farallon de Pajaros	1.34	13.36	133.6

Note the (very) slight increase in EPP-implied coordinate uncertainty in NATRF2022 as one moves northward (from point 7 to points 1 and 2), showing their slightly extra sensitivity to rotation, being further from the rotation pole (which lies due south of Mexico, just south of the equator) than other points chosen on that plate.

The particularly large uncertainties in the Caribbean(1) model and the Mariana model are highlighted in yellow.

3.1 Discussion

Formal error propagation has been performed on a variety of points on four plates, one for each of the terrestrial reference frames of the modernized NSRS. This means that two potential sources of NSRS coordinate uncertainty were considered:

1) Positioning uncertainty in the ITRF
2) Plate rotation uncertainty

The final, modernized NSRS Euler pole parameters (and their uncertainties) reflecting each of the four plate rotations are not currently known, but it is reasonable to assume that the values taken from the most recent and comprehensive studies of each of the four plates will be within the same general ballpark as the final NSRS values.

As such, certain conclusions can be drawn. The first is that, no matter how well the Euler pole parameters of the plate rotation are known, *if* they have any uncertainties whatsoever, those uncertainties *can* (formally) be propagated into the NSRS coordinates if one so chooses, using the blue portion of equation 10.

Second, the experiments bear out that positioning uncertainty in the ITRF will propagate 1:1 into the same positioning uncertainty when converted into the NSRS. That is:

$$\boldsymbol{\Sigma}_{\boldsymbol{Y_1}} = \boldsymbol{\Sigma}_{\boldsymbol{X_1}} \tag{17}$$

Finally, and most importantly, the size of the EPP-implied uncertainties must be considered. With the recent improved estimate of the Caribbean EPPs by Snay and Saleh (2020), the only significant source of EPP uncertainty within the modernized NSRS is expected to be for the Mariana plate. Table 1 implies that, if NGS were to formally adopt EPP-implied uncertainties as a source of ENU coordinate uncertainties in MATRF2022, that users could expect an additional 1.3 cm of total formal horizontal uncertainty for every year passed since 2020. That is, no matter how well a survey is performed in, say 2025, the final horizontal coordinate uncertainty would have an additional +/- 6.5 cm uncertainty. In 2030 that becomes +/- 13 cm.

Table 1 implies only sub-cm impacts in NATRF2022, PATRF2022 and CATRF2022 for a similar 2030 survey which seems reasonable, and has the advantage of being mathematically correct as well.

Therefore NGS must face a choice on whether to have a consistent or inconsistent policy. On the one hand, in 2030, having OPUS provide a GNSS user in the Marianas with a formal horizontal coordinate accuracy of over 1 decimeter, no matter how well the survey is performed, seems ridiculous on the face of it. On the other hand, the rotation of the Mariana plate is (relatively) poorly determined, and is likely to remain so for years to come. Is it not fair to reflect that ITRF2020 positioning is much more accurate than rotating into a poorly determined plate-fixed frame?

In order to shed just a bit more light on the subject, the two different situations of NATRF2022 and MATRF2022 are examined. Consider the Northern Alaska point in NATRF2022 (the most sensitive to errors in the North American EPPs) and the Guam point in MATRF2022 (the least sensitive to errors in the Mariana EPPs). Graphing their respective latitude determinations is shown in Figures 1 and 2.

In both figures, time runs along the X axis from 1920 to 2120. The ITRF2020 latitude is plotted in black, and the ±1 cm positioning uncertainty is plotted in parallel grey lines above and below it (scaled to differentiate the various lines).

This latitude is then converted to the NATRF2022 latitude (Figure 1) or the MATRF2022 latitude (Figure 2), shown in green on both figures. The ±1 cm positioning uncertainty (from ITRF2020), formally propagated into NATRF2022 or MATRF2022 positioning (only) uncertainty, is plotted in parallel blue lines above and below the green.

The combination of both positioning uncertainty (always ±1 cm in latitude) with EPP uncertainty (growing through time away from 2020), is shown in red. Note that in figure 1, the NATRF2022 *total* uncertainty is a very subtly growing value, rising from 1.0 cm (at 2020) to a total of 2.9 cm (1.0 cm from positioning, 2.7 cm from EPPs, combined in quadrature) over 100 years.

However, the MATRF2022 *total* uncertainty is a rapidly growing value, rising from 1.0 cm (at 2020) to a total of 51.7 cm (1.0 cm from positioning, 51.7 cm from EPPs, combined in quadrature) over 100 years.

When considering how to report uncertainties for the modernized NSRS, the decision comes down to choosing the blue line, or the red line, in Figure 1 and Figure 2.

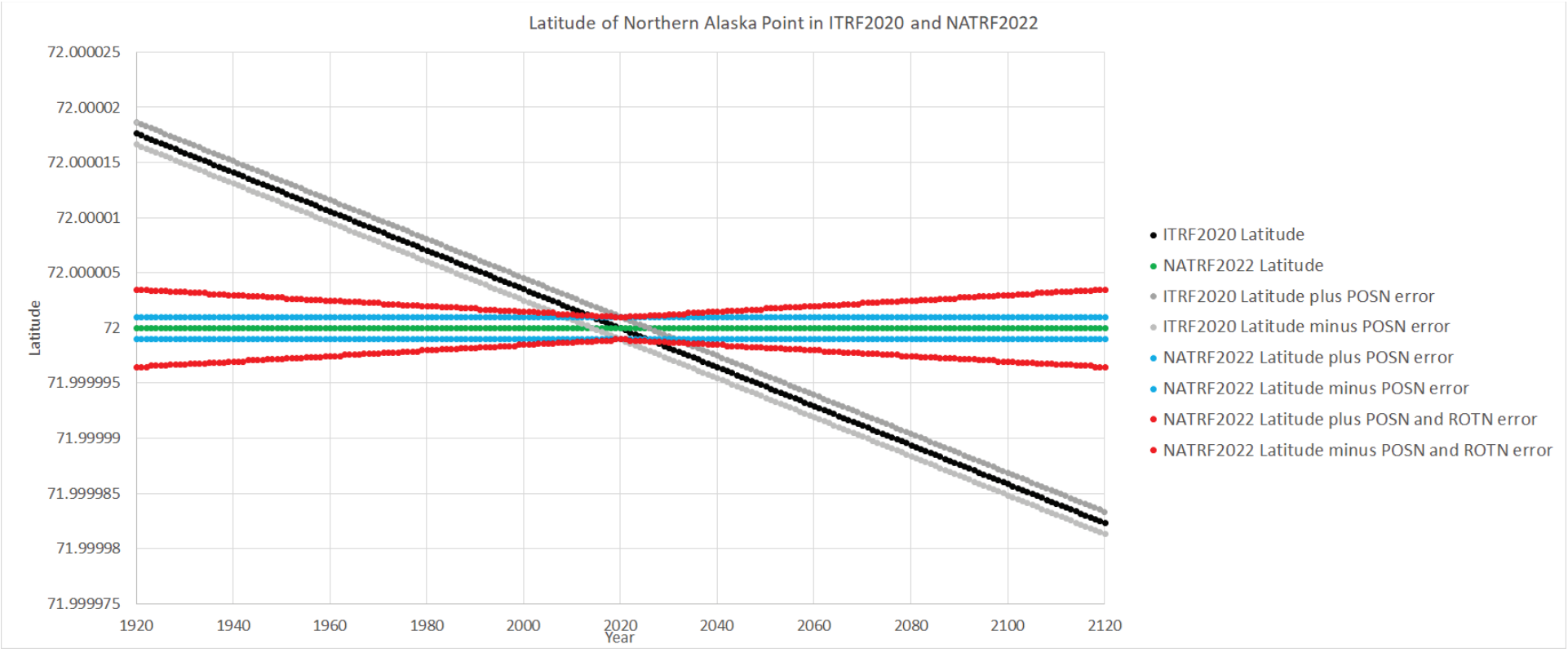

Figure 1: Latitude and uncertainty computations for N. Alaska. POSN and ROTN mean error from positioning and error from EPP uncertainty.

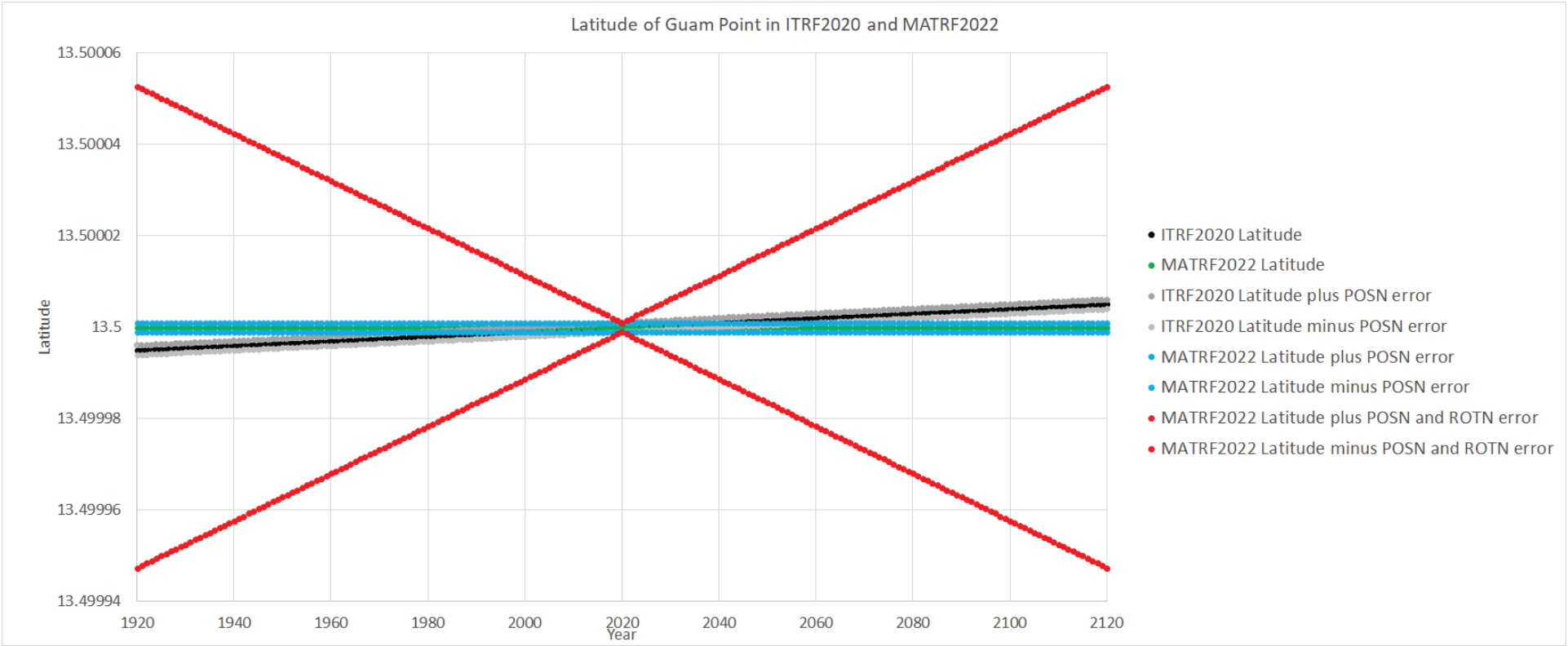

Figure 2: Latitude and uncertainty computations for Guam. POSN and ROTN mean error from positioning and error from EPP uncertainty.

3.2 Decision

NGS will choose both consistency and practicality over scientific perfection on the topic of propagating EPP-uncertainty into NSRS plate fixed coordinate uncertainty. While we will *compute* the propagated EPP uncertainty (and allow users access to this value if it suits their needs) the formal coordinate accuracy estimates of plate fixed NSRS coordinates provided by NGS (in software such as OPUS and from data in the NSRS database) in the modernized NSRS will *not* include the effect of EPP uncertainties.

Should the Mariana plate rotation EPPs be significantly improved in the future, this decision may be revisited. But for now, for consistency, the above policy will be applied to all four terrestrial reference frames of the modernized NSRS.

4 Bibliography

Altamimi, Z., L. Métivier and X. Collilieux, 2012: ITRF2008 plate motion model, *Journal of Geophysical Research*, v. 1179, B07402, pp. 1-14.

Altamimi, Z., L. Métivier, P. Rebischung, H. Rouby and X. Collilieux, 2017: ITRF2014 plate motion model, *Geophysical Journal International*, v. 209, pp. 1906-1912.

National Geodetic Survey, 2020: Blueprint for the Modernized NSRS, Part 1: Geometric Coordinates and Terrestrial Reference Frames, *NOAA Technical Report NOS NGS 62*.

Smith, D., 2020: A GPS-based Estimate of the rotation of the Mariana plate in both ITRF2008 and ITRF2014, *NOAA Technical Report NOS NGS 74.*
https://geodesy.noaa.gov/library/pdfs/NOAA_TR_NOS_NGS_0074.pdf

Snay, R. and J. Saleh, 2020: Expanding TRANS4D's Scope to Provide 3-D Crustal Velocity Estimates for a Neighborhood of the Caribbean Plate, *pre-publication copy*.